

DOI: 10.36297/vw.jei.v4i2.62

VW Engineering International, Volume: 4, Issue: 2, 50-58

Fabrication of Composites Based on ZA-27 Alloy Reinforced with Carbon Fiber and Graphite Particles in varying percentage.

Arsum Javaid^{*}, Anuj Kumar, Dheeraj Sagar, Himanshu Singh

Department of Mechanical Engineering, Invertis University, Bareilly 243123, India

^{*}Corresponding Author's Email: arsumjavaid08@gmail.com,

Received:
May 09, 2022
Accepted:
June 15, 2022
Published online:
June 15, 2022

Abstract: The purpose of this study is to see how carbon fiber and graphite reinforcement affects the strength, wear, hardness, etc. of the ZA-27 alloy. The stir casting process was used to create composites containing carbon fiber and graphite particles. Using a block-on-disk tribometer, the tribological characteristics of unreinforced alloys and composites were investigated at various specific loads and sliding speeds. In all combinations of applied loads (F_n) and sliding speeds (v) in testing, the ZA-27/graphite composite specimens displayed much lower wear performance than the matrix aluminum specimens. Nonuniform triboinduced graphite films were generated in test circumstances defined by a low graphite content and low sliding speeds and applied loads, resulting in a rise in the friction coefficient and wear rate as the sliding speed and applied load increased. It was found that reinforced samples performed better tribologically. Carbon fiber and graphite reinforced ZA-27 may find new applications in various machine parts in the industry.

Keywords: ZA-27 alloy, Carbon Fiber, Graphite particles, Fabrication, Tribological Behavior

1. Introduction

Composite technology has been heavily explored in recent times due to its vast range of possible uses [1]. Metal matrix composites (MMCs) have evolved as a significant class of sophisticated materials, allowing engineers to adapt material characteristics to their specific requirements [2]. During the 1980s, Al-based materials were reinforced using SiC particles, and Al₂O₃ molecules, with the focus on spatially separated reinforced metal composites. They are appealing for a variety of applications due to a combination of superior characteristics, low cost, and great machinability [3]. Zinc-aluminum (ZA) alloys are significant bearing elements that are particularly well suited to high-load, low-speed tasks [4]. The ZA alloys (mostly ZA-12 and ZA-27) are able to substitute aluminum cast composite materials and bearing brass, as well as cast iron, plastic materials, or even steels for production tribo-elements for reasonable exploitation

temperature changes, due to their good tribo-mechanical properties, low weight, excellent foundry castability and fluidity, good machining properties, low initial cost, and eco-friendly techniques.

These features have inspired scholars to strengthen them using various dispersed reinforcing materials in order to achieve significantly improved mechanical performances. As a result, MMCs built on the ZA matrix have become increasingly popular as gentle and surface roughness materials is important. The introduction of hard particles (namely Carbon Fibers and Graphite) greatly increases the sliding and resistance properties of granular reinforced Zn-Al composites, according to several researchers [2] [2], [5], [14]-[16], [6]-[13]. When compared to unreinforced ZA-27 alloy specimens during unlubricated [5] and lubricated sliding [6]. SiC-reinforced materials had a

lower wear rate. The rate of wear reduced as the SiC concentration increased. Zircon particles [14], garnet particles [15], and short glass fibers [17] all had comparable outcomes. In addition, Prepared particles reinforcing increased the abrasive wear performance of matrix zinc-based alloys [14], [15], [17]. In recent years, much research has focused on graphite.

Efforts were made in the hopes of developing a material with low friction, low wear rate, and superior capabilities. Graphite in Al alloy MMCs has been shown to improve the tribological characteristics of the composites during dry sliding by forming a self-lubricating graphite-rich coating on the area of contact [18]–[21]. The characteristics of Zn–Al alloy/graphite particle composites, have not been explored as thoroughly. The mechanical property of the ZA-27 Zinc–aluminum alloy/Graphite particle composites were shown to be strongly affected by the quantity of graphite used as well as the heating [22]–[24]. The procedure, reinforcing thickness, filler content and redistribution, as well as the cutting speed, applied stress, and environmental conditions, all have a tribological impact on the construction of an ideal ZA-27/graphite carbon fiber composite. As a result, the stir casting process was employed to make ZA-27 composites reinforced with Carbon Fiber and Graphite particles in this work. An effort was made to assess the composite's dry and greased sliding frictional behavior over a variety of design forces and sliding velocities. As a reference data, the unreinforced ZA-27 alloy was examined. The role of graphite was examined in both dry and greased situations.

2. Experimental Procedure:

2.1 Preparation of the Composite:

As the basis matrix metal, the ZA-27 was employed. As reinforcement, graphite particles and Carbon Fiber particles were utilized. The Carbon Fiber & Graphite contents were (0%:0%), (3%:2%), (6%:4%), (9%:6%) respectively by weight. The hybrid samples were produced using the Stir Casting method, which involved mixing in a homogeneous environment with the help of a stirrer. A lab electric 2-kW resistance furnace (with temperature control) and a laboratory stirrer are used in the stir casting process [5]. Through the tiny aperture in the furnace wall, the thermocouple was placed 20 mm above the bottom of the cast iron crucible. The recording and modification of the mixing rate was done by using the electronic equipment i.e., laboratory stirrer and thermocouples that were installed. Table 1. shows the chemical composition of the ZA-27 alloy.

Table 1 Chemical Composition of ZA-27

Chemical Composition of ZA-27 (weight %)				
Al	Cu	Mg	Fe, Sn, Cd, Pb	Zn
25-27	2-2.5	0.015-0.02	Trace Qty.	Balance

The preparation of the samples was done at a furnace shop in Moradabad.



Figure 1 Stir Casting with Laboratory Stirrer

The materials were dissolved in the electrical component furnace's previous heated vessel (around 600°C). The melt was then elevated to 990°C (to properly melt copper, which has comparatively high melting point.). Additional slag was also removed at this high temperature. After that, the crucible was cooled to 485°C, which was the combining point. After the laboratory stirrer was brought in, the mixing began (from 0 to 600 RPM) while the melt was simultaneously cooled to 462°C, the working range for the stir casting method. After reaching the desired thermal resistance and RPMs, the semi-solidified melt was subjected to isothermal isotropic process for 5 minutes, in order to eliminate the dendritic morphology and prepare the melt for penetration. Figure 2 shows a ZA-27 sample prepared after stir casting.



Figure 2 ZA-27 Sample prepared after Stir Casting.

The known volume of carbon fiber and graphite respectively was warmed in the furnace at roughly 150°C before mixing in composite to remove moisture. At 200 RPMs, Carbon fiber was injected in up for 3 minutes, right adjacent to the mixer's shaft. Similarly,

graphite was also mixed in the composite. Following the completion of the reinforcement, the speed of stirrer (RPMs) was steadily raised over the following 2 minutes, eventually reaching the working number of 600 RPMs. The carbon fiber and graphite particles were then isothermally "mixed-in" into the semi-solidified melt of ZA-27 for the aim of homogenization, i.e., to get better particle sizes, during the following 30 minutes at workplace practices of 600 RPMs and 462°C.

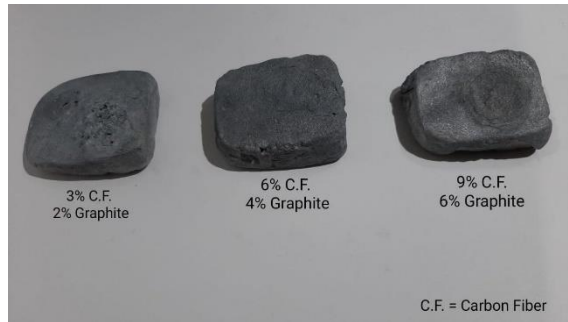


Figure 3 Reinforced samples with varying proportions.

Methodology

Table 2 Amounts of Different Elements Used to make composite (in grams)

Al	Mg	Cu	Pb	Cd	Sn	Zn
1080	0.6	3	0.24	0.24	0.12	2915

The following tests have been performed on the reinforced composite samples. Table 2 illustrates the different weights (in grams) taken of the constituent elements in the making of different composite samples.

2.2 XRD or X-Ray Diffraction:

XRD or X-Ray Diffraction test is conducted to study the crystal structure of any material. It is conducted by focusing an X-Ray beam on the given specimen. After this, the amount of scattering is measured in terms of the outgoing direction of the beam. Now, this scatter, also known as the diffraction pattern, displays the sample's crystalline structure once the beam is split. Most of the samples tested are prepared as finely ground powder and evaluated using powder diffraction.

X-Ray Diffraction tests were performed in CSIR-CBRI, Roorkee. Figure 4 shows samples in powdered form which were used for testing under the X-Ray diffraction machine.

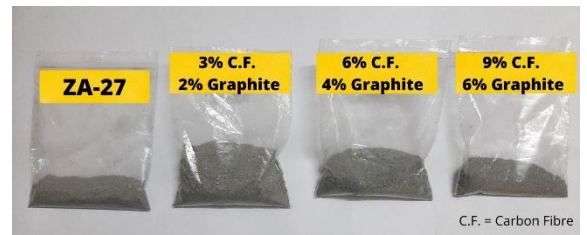


Figure 4 Powdered Specimen for X-Ray Powder Diffraction

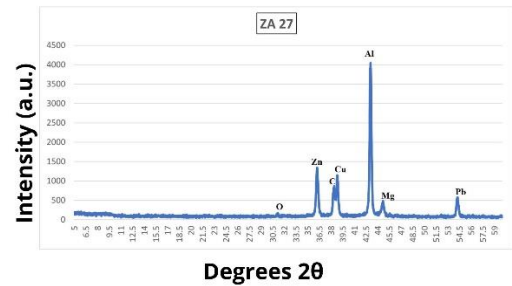


Figure 5 XRD Result for ZA-27 sample.

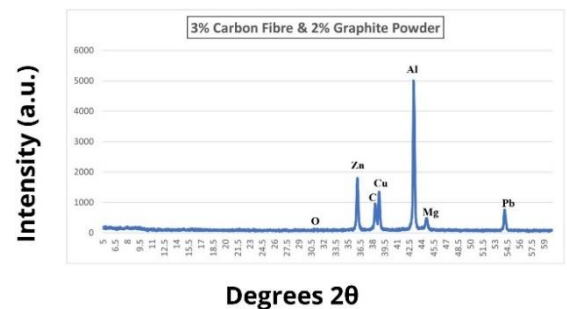


Figure 6 XRD Result for 3% C.F. & 2% Graphite composite.

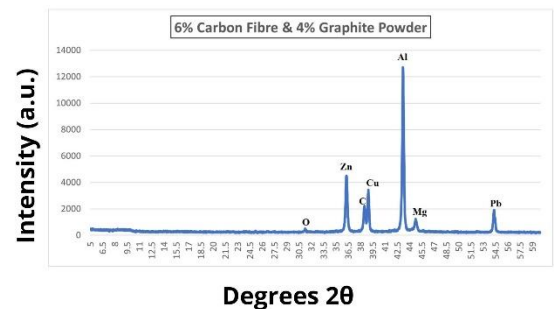


Figure 7 XRD Result for 6% C.F. & 4% Graphite composite.

Figure 5 shows the X-Ray Diffraction results for the ZA-27 reference sample.

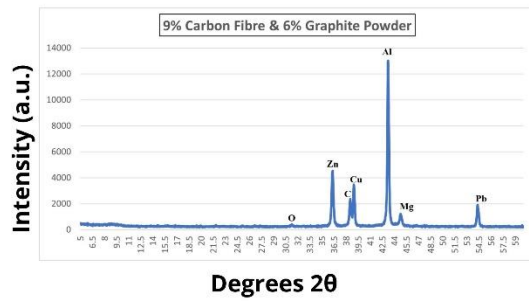


Figure 8 XRD Result for 9% C.F. & 6% Graphite composite.

Figures 6-8 show the presence of different elements present in the different reinforced composite samples. Here, X-axis represents the angle of the diffracted beam, measured in degrees (2θ). Whereas, Y-axis represents the intensity of the diffracted beam, measured in arbitrary units.

2.3 Wear Analysis (Using Pin on Disk)

This test is performed to analyze the wear properties of the samples using pins of samples sliding on a disc rotating on a predefined set of RPMs of the disc and different forces exerted in the pin under different weights (loads). Figures 9-11 show the wear test (Pin-on-disk) machine from various angles.



Figure 9 Pin-on-disk test machine



Figure 10 Digital Control Panel (Wear Test Apparatus)



Figure 11 Rotating Disk in dry sliding conditions.

Sample size of the pins is taken to be 10 mm in diameter and 25.4 mm in length. Figure 12 shows the pins prepared for Pin-on-disk wear testing. These pins are carved out from the samples using a Lathe machine in a workshop in Moradabad, Uttar Pradesh.



Figure 12 Composite pins for wear test

2.4 Taguchi L16 Orthogonal Array

To reduce number of iterations, and substantially improve experiment results efficiently, Taguchi L16 orthogonal array was utilized using a computation software named MiniTab.

Genichi Taguchi, who invented this method, was a Japanese engineer. In this method, one has to performed the experiments only 16 times, which is comparatively much less than hundreds of cumbersome tests. The results of wear test are explained in tabular form in Table 3.

Pin On Disk test is performed at Tribology Lab of MJP Rohilkhand University, Bareilly, Uttar Pradesh.

2.5 Brinell's Hardness Test

All of the specimens' hardness was determined using a Brinell hardness tester with a 2.5-mm steel ball indenter and an 875N applied force. It took 60 seconds to apply the load. Seah discovered that when the graphite concentration in ZA-27 composites increases, the tensile strength of the composites reduces steadily over time [23]. In fact, as the graphite percentage rises from 0% to 5%, the hardness value falls by about 27%.

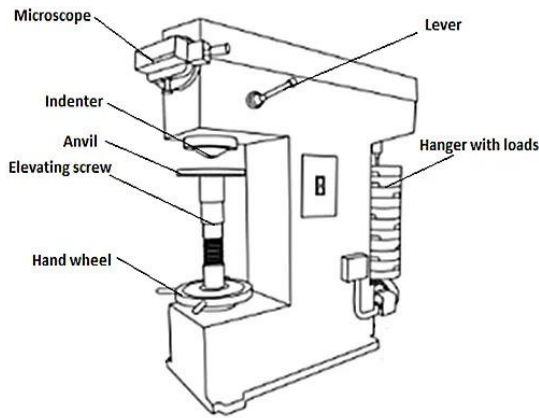


Figure 13 Schematic arrangement of Brinell's Hardness Testing Machine

The samples were put through their paces on a digital pin-on-disk sliding wear testing system with contact pair geometry that followed ASTM G 77-83 standards. Figure 13 depicts the test machine's basic design. There is a more detailed explanation of the tribometer elsewhere [26]. The carbon fiber and graphite strengthened ZA-27 alloy composite and as-cast ZA-27 alloy were used to make the test blocks. Their contact surfaces were polished. The experiments were conducted at various sliding speeds (1.00-2.50 m/s) and applied loads (25-100 N) in both lubricated and dry situations. Each process was repeated 3 times.

2.6 Formula for calculating Brinell Hardness Number.

$$HB = \frac{2P}{\pi D(D - \sqrt{D^2 - d^2})}$$

Where, HB = Brinell's Hardness Number (kg/mm²)

P = load in kgf

D = steel ball diameter in mm

d = indentation diameter in mm

The period of slipping in the first set of tests was 60 minutes for lubricated circumstances and 10 minutes for dry sliding settings. To gather data for the fatigue curves, the tests were done with periodic stops of the friction process for wear measurements. The remainder of the tests were run in a continuous loop with a constant sliding distance. The experiments were carried out at room temperature. During the lubricated testing, the discs were continually submerged in 25 mL of lubricant up to a depth of 2 mm. The block's wear behavior was measured in terms of wear scar width. For duplicate testing, the reliability of the results was determined to be good.

After the Brinell Hardness Test, the following results were found, which are shown in Table 4.

Table 3 Hardness Numbers for Reinforced Samples.

S. No.	Sample	BHN
1	ZA-27 (Matrix Alloy)	117
2	3% C. F. & 2% Graphite	118
3	6% C. F. & 4% Graphite	119
4	9% C. F. & 6% Graphite	120

2.7 Density (Using Archimedes' Principle)

The density of the ZA-27/carbon fiber, graphite composite was 4.74 g/cm³ as measured by Archimedes' principle. The weight was measured to a precision of 0.1 mg on a spring balance. When compared to the average density of 4.9 g/cm³, the observed density was less. The ZA-27 alloy, carbon fiber particles, graphite particles were calculated to have densities of 5.0 g/cm³, 1.6 g/cm³ and 2.2 g/cm³, respectively. The gap between the observed and computed density values allowed a porosity volume percentage of 4.1 percent to be determined. Figure 14 demonstrates calculating of density using the Archimedes' principle.

1	Reinforcement	Load (N)	Distance (m)	Speed (m/s)	Speed (rpm)	Time (s)	W1 (g)	W2 (g)	w1-w2 (g)
2	0	25	500	1	120	500	9.48	9.26	0.22
3	0	50	1000	1.5	180	660	9.26	8.98	0.28
4	0	75	1500	2	240	750	8.98	8.67	0.31
5	0	100	2000	2.5	300	800	8.67	8.44	0.23
6	A	25	1000	2	240	500	9.56	9.32	0.24
7	A	50	500	2.5	300	200	9.32	9.03	0.29
8	A	75	2000	1	120	2000	9.03	8.88	0.15
9	A	100	1500	1.5	180	1000	8.88	8.65	0.23
10	B	25	1500	2.5	300	600	10.34	10.22	0.12
11	B	50	2000	2	240	1000	10.22	9.98	0.24
12	B	75	500	1.5	180	330	9.98	9.65	0.33
13	B	100	1000	1	120	1000	9.65	9.39	0.26
14	C	25	2000	1.5	180	1330	10.16	9.96	0.2
15	C	50	1500	1	120	1500	9.96	9.73	0.23
16	C	75	1000	2.5	300	400	9.73	9.56	0.17
17	C	100	500	2	240	250	9.56	9.27	0.29

Table A: Taguchi L16 Array for Wear Test

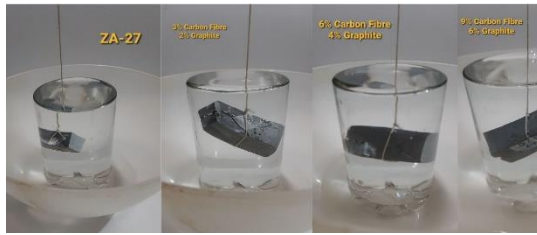


Figure 14 Calculating Density using Archimedes' Principle.

	Sample	Weight	Apparent Weight	Density (g/cm ³)
1	ZA-27	28	22	4.74
2	3% A ¹ , 2% B ²	62	50	4.93
3	6% A, 4% B	76	61	5.05
4	9% A, 6% B	46	37	5.16

Table 4 Density Calculation Table

3. Results And Discussion

The wear behavior of the studied compounds was often characterized by intense wear during the first minutes of sliding, followed by a steady state phase. When contrasted to the matrix ZA-27 alloy, the wear of the composites containing carbon fiber & graphite particles was always much lower.

It can be shown that under dry sliding circumstances, wear is substantially higher than in lubricated sliding. The rises with applied load at evaluated sliding velocity (1.5, 2.0, and 2.5 m/s), with the matrix alloy showing a particularly high rate of wear in the lubricated sliding circumstances. For greased and dry wear testing, the nature of the sliding speed impact on wear is different. The wear rate of both the base alloy and the composite specimens reduced as the sliding speed increased in the first scenario. Whereas, in dry sliding, increasing the sliding speed induces an increase in the wear rate. The particular mechanical and thermal stresses of materials are exceptionally high, resulting in extensive run-in wear at the start of the friction process. The contact area rises as the sliding process continues, whereas the true contact pressure reduces drastically. This is followed by a drop in wear intensity. The specified run-in process is accompanied by a change in the degree of friction coefficient. The initial decline in the friction coefficient may be seen in the case of friction with lubrication. When it comes to dry friction, it's obvious that the friction coefficient rises as the sliding process progresses.

In the case of matrix alloy, the rise is more pronounced than in the case of composite. It was also observed that

the matrix alloy has the greatest friction coefficient throughout the friction process. The steady state friction coefficient of the investigated materials as a function of applied load at different sliding speeds under lubricated and dry conditions. In dry sliding circumstances, the friction coefficient is substantially larger than in lubricated sliding situations. The friction coefficient of the matrix alloy, as well as the composite, rises with applied load at all sliding speeds.

In lubricated sliding, the friction coefficient reduced as the sliding speed increased. In dry sliding, the coefficient of friction rose as the sliding speed increased. The decreasing friction coefficient in lubricated tests with increasing sliding speed and decreasing applied load indicate that friction was occurring in boundary and mixed lubrication regimes.

In general, composite specimens had a lower wear rate and coefficient of friction than matrix alloy specimens for all combinations of applied loads and sliding speeds in both lubricated and dry sliding circumstances. The wear resistance between the composite and the matrix alloy grew as the applied load increased. This increase was mild in dry sliding circumstances, but it was quite noticeable in lubricated sliding situations.

When it comes to antifriction qualities, the advantage of composite over matrix alloy is more pronounced in the region of greater applied loads and sliding speeds. The creation of a graphite-rich coating on the tribo-surface, which offers solid lubrication, might explain this tribological enhancement.

In graphite's hexagonal structure, strong chemical bonds between atoms create strong interatomic bonds within a plane, whereas bonding is relatively weak in a direction perpendicular to these planes. Graphite also forms strong chemical interactions when it combines with gases. The crystalline platelets are easily sheared and transferred to the contact surfaces as a result [27].

In graphite's hexagonal structure, strong chemical bonds between atoms create strong interatomic bonds within a plane, whereas bonding is relatively weak in a direction perpendicular to these planes. Graphite also forms strong chemical interactions when it combines with gases. The crystalline platelets are easily sheared and transferred to the contact surfaces as a result [27].

The smearing process, according to Liu et al.[29], takes time to properly develop a layer of graphite that will cover almost whole contact surface. In general, the formation speed of protective tribo-layers is proportional to the sliding speed, contact stresses, and graphite concentration of the composite. Rihahi and Alpas [19] discovered that the contact surface of a

¹ A = Carbon Fibre. ¹ B = Graphite.

graphitic aluminum matrix composite with 4% graphite was 40% covered by the tribo-layer at a slow sliding speed (0.5 m/s) and a light load (10 N).

The fraction of the contact surface area covered by tribo-layers rose as sliding speed and load increased. Yang et al. [20] discovered that in composites with 2% graphite, there is insufficient lubricating coating of graphite to prevent direct contact of surfaces owing to minor sliding speeds, resulting in wear rate rise with sliding speed.

Our experiments were carried out using an Al-27/graphite composite having just 2% graphite at low sliding speeds (0.26–1.0 m/s) and applied loads (10–80 N). In lubricated sliding, the self-lubricating effect of graphite reinforcing particles is also highly important. The good tribological effects of graphite in lubricated sliding can be attributed to its influence on the tribological features of the lubricating oil. Sharma et al. [27] validated the good impacts of graphite on improving the tribological behavior of the ZA-27 alloy in his tests on the bearing formed of the ZA-27/graphite composite.

Prasad also performed a lubricated pin-on-disk wear test on a zinc-based alloy reinforced with SiC particles and looked into the influence of varied quantities of graphite on the tribological features of lubricating oil in boundary lubrication circumstances [30]. With a lower concentration of graphite in the lubricating oil, he discovered that good effects of graphite additions to the lubricating oil in lowering the friction coefficient of the tested composite in boundary lubrication could be accomplished (up to 4% by weight). The reversal trend was produced by a greater quantity of graphite in the lubricant mixture.

Under the applied force, graphite shears into very small particles, which mix with the oil being drawn from the reservoir by the revolving disc. The findings show that the degree of graphite's favorable impact on the tribological behavior of composites is dependent on the contact circumstances.

With increasing applied load and sliding speed, variations in tribological parameters between the composite and matrix alloy rise in %. This is due to the effect of the sliding speed and applied stress on the graphite release rate that was previously described. The concentration of graphite particles in the lubricating oil increases as the amount of released graphite grows, enhancing the lubricating fluid's tribological qualities.

The graphite coating decreases direct contact with surfaces in the boundary lubrication regime, which is expressed by decreased wear rate and friction coefficient. In addition, in composites, due to the graphite layer, the shift into the mixed lubrication

regime occurs at lower v/F_n ratios than in the matrix alloy.

4. Conclusions

In all permutations of applied loads, sliding speeds, and test conditions, the ZA-27/graphite composite specimens displayed better tribological properties than the matrix alloy specimens, despite their lower hardness.

The creation of the graphite rich coating on the tribo-surface, which offers solid lubrication, might explain the favorable benefits of carbon fiber and graphite reinforcement in dry sliding. In such circumstances, full separation of the contact surfaces was not guaranteed, resulting in a rise in friction coefficient and wear rate as the sliding speed and applied load increased. Despite the fact that the tribo-induced graphite coating was not homogeneous, it permitted a lower chance of direct metal-to-metal contact, lowering the wear rate and coefficient of friction substantially.

The impact of graphite on tribological features of lubricating oil can be linked to its favorable function in lubricated wear tests. The lubricating oil interacted with the tribo-induced graphite to generate an emulsion with increased tribological properties.

The intensity of the graphite release is influenced by the sliding speed and applied stress. When it comes to ZA-27, this is reflected by the composite wear rate and friction coefficient's decreased sensitivity to the negative effect of the applied load, as well as their enhanced sensitivity to the positive influence of sliding speed.

Author Contributions: Arsum Javaid, conceptualized the idea of synthesizing composites of ZA-27 alloy with the guidance of Anuj Kumar and Dheeraj Sagar. Himanshu Singh help conduct background research for the project. **Conceptualization,** Arsum Javaid and Anuj Kumar; **methodology,** Arsum Javaid; **software,** Himanshu Singh; **Validation,** Anuj Kumar, Dheeraj Sagar and Tauseef Siddiqui; **Formal Analysis,** Arsum Javaid; **Resources,** Arsum Javaid and Himanshu Singh; **Writing—original draft preparation,** Arsum Javaid; **Writing—review and editing,** Arsum Javaid and Himanshu Singh; **Visualization,** Himanshu Singh; **supervision,** Anuj Kumar.

All authors have read and agreed to the published version of the manuscript.

Funding: This research received no external funding and all the expenses were borne by Arsum Javaid and Himanshu Singh.

Acknowledgments: Thanks to various laboratories, guides, professors, workshops in various cities which played a vital role in the completion of this project. The list includes but not limited to:

- A) **Anuj Kumar**, Asst. Professor, Invertis University, Bareilly for his valuable guidance at every step of the project, without which this work would not have been possible.
- B) **Dheeraj Sagar**, Asst. Professor, Invertis University, Bareilly for opening lines for various communications, helping conduct background research, etc.
- C) **Tauseef Siddiqui**, Asst. Professor, MJP Rohilkhand University, Bareilly who facilitated the use of Tribology Lab.
- D) **Tabish Alam**, Scientist, CSIR-CBRI, Roorkee for letting us use the X-Ray Diffraction Machine for powdered X-RD.
- E) **Himanshu Singh**, BTech +MTech (ME), Invertis University, Bareilly, for constantly providing resources, finding materials, and being a bridge for the experimental work.

Conflicts of Interest: I, Arsum Javaid, as the first author, declare no conflict of interest. Other authors, i.e., Himanshu Singh, Anuj Kumar, Dheeraj Sagar helped in the design of the study; in the collection, analyses, and interpretation of data; in the writing of the manuscript, and to publish the results.

References:

- [1] E. Vasiliev, V.V., Morozov, "Mechanics and Analysis of Composite Materials," *Oxford*, 2001, [Online]. Available: https://books.google.co.in/books?hl=en&lr=&id=tpwe5y10AIwC&oi=fnd&pg=PP1&dq=Mechanics+and+Analysis+of+Composite+Materials&ots=IHhvi7rUVVQ&sig=hWwkbqsv0EXWm2Tx7sIN4gLYyZ8&redir_esc=y#v=onepage&q&f=false
- [2] B. K. Prasad, "Abrasive wear characteristics of a zinc-based alloy and zinc-alloy/SiC composite," *Wear*, vol. 252, no. 3-4, pp. 250-263, Feb. 2002, doi: 10.1016/S0043-1648(01)00872-9.
- [3] P. Cahn, R.W., Haasen, "Physical Metallurgy, 4th edn. NorthHolland," *Amsterdam*, p. 89875, 1996, [Online]. Available: <https://www.elsevier.com/books/physical-metallurgy/cahn/978-0-444-89875-3>
- [4] A. R. Miroslav BABIC, Rato Ninkovic, "Sliding Wear Behavior Of Zn-Al Alloys In Conditions Of Boundary Lubrication," *Ann. Univ. "Dunarea Jos" Galati Fascicle VIII. Tribol.*, pp. 60-64, 2005.
- [5] S. C. Sharma, B. M. Girish, R. Kamath, and B. M. Satish, "Effect of SiC particle reinforcement on the unlubricated sliding wear behaviour of ZA-27 alloy composites," *Wear*, vol. 213, no. 1-2, pp. 33-40, 1997, doi: 10.1016/S0043-1648(97)00185-3.
- [6] S. C. Tjong and F. Chen, "Wear behavior of As-cast ZnAl27/SiC particulate metal-matrix composites under lubricated sliding condition," *Metall. Mater. Trans. A Phys. Metall. Mater. Sci.*, vol. 28 A, no. 9, pp. 1951-1955, 1997, doi: 10.1007/s11661-997-0127-1.
- [7] B. K. Prasad, S. Das, A. K. Jha, O. P. Modi, R. Dasgupta, and A. H. Yegneswaran, "Factors controlling the abrasive wear response of a zinc-based alloy silicon carbide particle composite," *Compos. Part A Appl. Sci. Manuf.*, vol. 28, no. 4, pp. 301-308, Jan. 1997, doi: 10.1016/S1359-835X(96)00115-7.
- [8] B. K. Prasad, O. P. Modi, and H. K. Khaira, "High-stress abrasive wear behaviour of a zinc-based alloy and its composite compared with a cast iron under varying track radius and load conditions," *Mater. Sci. Eng. A*, vol. 381, no. 1-2, pp. 343-354, Sep. 2004, doi: 10.1016/J.MSEA.2004.04.030.
- [9] J. Sastry, S., Krishna, M., Uchil, "A study on damping behavior of aluminate particulate reinforced ZA-27 alloy metal matrix composites," *J Alloy. Compd* 346, pp. 268-274, 2001.
- [10] S. C. Sharma, S. Sastry, and M. Krishna, "Effect of aging parameters on the micro structure and properties of ZA-27/aluminate metal matrix composites," *J. Alloys Compd.*, vol. 346, no. 1-2, pp. 292-301, 2002, doi: 10.1016/S0925-8388(02)00528-5.
- [11] I. Bobić, M. T. Jovanović, and N. Ilić, "Microstructure and strength of ZA-27-based composites reinforced with Al₂O₃ particles," *Mater. Lett.*, vol. 57, no. 11, pp. 1683-1688, Mar. 2003, doi: 10.1016/S0167-577X(02)01052-2.
- [12] O. P. Modi, S. Rathod, B. K. Prasad, A. K. Jha, and G. Dixit, "The influence of alumina particle dispersion and test parameters on dry sliding wear behaviour of zinc-based alloy," *Tribol. Int.*, vol. 40, no. 7, pp. 1137-1146, 2007, doi: 10.1016/j.triboint.2006.11.004.
- [13] K. Yu, S., He, Z., Chen, "Dry sliding frictional wear behavior of short fibre reinforced zinc-based alloy composites," *Wear* 198, vol. 66, no. November, pp. 108-114, 1996.
- [14] S. C. Sharma, B. M. Girish, D. R. Somashekar, B. M. Satish, and R. Kamath, "Sliding wear behaviour of zircon particles reinforced ZA-27 alloy composite materials," *Wear*, vol. 224, no. 1, pp. 89-94, Jan. 1999, doi: 10.1016/S0043-1648(98)00334-2.
- [15] G. Ranganath, S. C. Sharma, and M. Krishna, "Dry sliding wear of garnet reinforced zinc/aluminium metal matrix composites," *Wear*, vol. 251, no. 1-12, pp. 1408-1413, Oct. 2001, doi: 10.1016/S0043-1648(01)00781-5.

- [16] S. C. Sharma, B. M. Girish, B. M. Satish, and R. Kamath, "Aging Characteristics of Short Glass Fiber Reinforced ZA-27 Alloy Composite Materials," *J. Mater. Eng. Perform.*, vol. 7, no. 6, pp. 747-750, 1998, doi: 10.1361/105994998770347305.
- [17] S. C. Sharma, B. M. Satish, B. M. Girish, R. Kamath, and H. Asanuma, "Dry sliding wear of short glass fibre reinforced zinc-aluminium composites," *Tribol. Int.*, vol. 31, no. 4, pp. 183-188, Apr. 1998, doi: 10.1016/S0301-679X(98)00020-6.
- [18] P. K. Rohatgi, S. Ray, and Y. Liu, "Tribological properties of metal matrix-graphite particle composites," *Int. Mater. Rev.*, vol. 37, no. 1, pp. 129-152, Jan. 1992, doi: 10.1179/imr.1992.37.1.129.
- [19] A. R. Riahi and A. T. Alpas, "The role of tribo-layers on the sliding wear behavior of graphitic aluminum matrix composites," *Wear*, vol. 251, no. 1-12, pp. 1396-1407, Oct. 2001, doi: 10.1016/S0043-1648(01)00796-7.
- [20] J. B. Yang, C. B. Lin, T. C. Wang, and H. Y. Chu, "The tribological characteristics of A356.2Al alloy/Gr(p) composites," *Wear*, vol. 257, no. 9-10, pp. 941-952, Nov. 2004, doi: 10.1016/J.WEAR.2004.05.015.
- [21] F. Akhlaghi and A. Zare-Bidaki, "Influence of graphite content on the dry sliding and oil impregnated sliding wear behavior of Al 2024-graphite composites produced by in situ powder metallurgy method," *Wear*, vol. 266, no. 1-2, pp. 37-45, Jan. 2009, doi: 10.1016/J.WEAR.2008.05.013.
- [22] K. H. W. Seah, S. C. Sharma, and B. M. Girish, "Mechanical properties of cast ZA-27/graphite particulate composites," *Mater. Des.*, vol. 16, no. 5, pp. 271-275, Jan. 1995, doi: 10.1016/0261-3069(96)00001-5.
- [23] K. H. W. Seah, S. C. Sharma, and B. M. Girish, "Effect of artificial ageing on the hardness of cast ZA-27/graphite particulate composites," *Mater. Des.*, vol. 16, no. 6, pp. 337-341, Jan. 1995, doi: 10.1016/0261-3069(96)00014-3.
- [24] K. H. W. Seah, S. C. Sharma, and B. M. Girish, "Corrosion characteristics of ZA-27-graphite particulate composites," *Corros. Sci.*, vol. 39, no. 1, pp. 1-7, Jan. 1997, doi: 10.1016/S0010-938X(96)00063-7.
- [25] A. Vencl, I. Bobić, M. T. Jovanović, M. Babić, and S. Mitrović, "Microstructural and tribological properties of A356 Al-Si alloy reinforced with Al₂O₃ particles," *Tribol. Lett.*, vol. 32, no. 3, pp. 159-170, 2008, doi: 10.1007/s11249-008-9374-6.
- [26] B. Miroslav, A. Vencl, S. Mitrović, and I. Bobić, "Influence of T4 heat treatment on tribological behavior of Za27 alloy under lubricated sliding condition," *Tribol. Lett.*, vol. 36, no. 2, pp. 125-134, 2009, doi: 10.1007/s11249-009-9467-x.
- [27] S. C. Sharma, B. M. Girish, R. Kamath, and B. M. Satish, "Graphite particles reinforced ZA-27 alloy composite materials for journal bearing applications," *Wear*, vol. 219, no. 2, pp. 162-168, Sep. 1998, doi: 10.1016/S0043-1648(98)00188-4.
- [28] K. H. W. Seah, S. C. Sharma, B. M. Girish, and S. C. Lim, "Wear characteristics of as-cast ZA-27/graphite particulate composites," *Mater. Des.*, vol. 17, no. 2, pp. 63-67, Jan. 1996, doi: 10.1016/S0261-3069(96)00033-7.
- [29] Y. B. Liu, S. C. Lim, S. Ray, and P. K. Rohatgi, "Friction and wear of aluminium-graphite composites: the smearing process of graphite during sliding," *Wear*, vol. 159, no. 2, pp. 201-205, Dec. 1992, doi: 10.1016/0043-1648(92)90303-P.
- [30] B. K. Prasad, "Investigation into sliding wear performance of zinc-based alloy reinforced with SiC particles in dry and lubricated conditions," vol. 262, pp. 262-273, 2007, doi: 10.1016/j.wear.2006.05.004.



© 2022 by the authors. Open access publication under the terms and conditions of the Creative Commons Attribution (CC BY) license (<http://creativecommons.org/licenses/by/4.0/>)